

Modification of a Previously Described Arteriovenous Malformation Model in the Swine: Endovascular and Combined Surgical/Endovascular Construction and Hemodynamics

Ralf Siekmann, Ajay K. Wakhloo, Baruch B. Lieber, Matthew J. Gounis, Afshin A. Divani, and L. Nelson Hopkins

BACKGROUND AND PURPOSE: The rete mirabile in swine has been proposed as an arteriovenous malformation (AVM) model for acute experimental studies through surgical creation of a large carotid-jugular fistula. This report describes two endovascular modifications to simplify the surgical creation and provides hemodynamic parameters for the AVM model.

METHODS: An AVM model was created in 29 animals to study n-butyl 2-cyanoacrylate polymerization kinetics. The common carotid artery (CCA) was punctured and a guiding catheter was inserted tightly into the origin of the ascending pharyngeal artery (APA). The CCA was ligated proximal to the catheter to create a pressure drop across the rete, which represented the AVM nidus. The catheter hub was opened whenever needed and served as the venous drainage of the AVM nidus. The contralateral APA served as the arterial feeder. Instead of the surgical ligation of the CCA, a temporary balloon occlusion was performed in three animals.

RESULTS: A mean pressure gradient of 14.9 ± 10.5 mm Hg (range, 4–42 mm Hg) was measured across the rete. The mean flow rate was 30.4 ± 14.2 mL/min (range, 3.5–46 mL/min), as measured at the venous drainage.

CONCLUSION: The endovascular and combined surgical-endovascular rete AVM model in swine is easy to construct and is less time-consuming than are the currently used models for acute experimental studies. Hemodynamic parameters can be monitored during the entire experiment and correspond to values found in human cerebral AVMs.

The endovascular treatment of arteriovenous malformations (AVMs) remains an art owing to the complexity of the AVM nidus, the supplying arterial feeders, and draining veins. Since its introduction in 1994 (1), the AVM model in swine has been widely used for research as well as for training and

education (2–7). This model uses both the left and the right parts of the swine's rete mirabile, a fine vascular network that supplies the cerebral arteries. It has some similarities to a plexiform human AVM. Surgical construction of one common carotid to a jugular vein fistula through a large side-to-side anastomosis facilitates the flow across the rete (Fig 1A). Subsequently, an endovascular occlusion of several ipsilateral branches and ligation of the ipsilateral common carotid artery are necessary to create the pressure drop required for the "arterio-arterial" shunt in the model.

The goal of our study was to simplify the existing combined surgical and endovascular construction of the AVM model in swine and to evaluate hemodynamic parameters before the planned embolization of the AVM.

Methods

All animal experiments were conducted in accordance with the policies set by the local University Institutional Animal Care and Use Committee (IACUC). Twenty-nine swine (four Mini Yucatan and 25 Barnyard) were used. The animals were

Received December 15, 1999; accepted after revision April 4, 2000.

From the Toshiba Stroke Research Center, Department of Neurosurgery (R.S., A.K.W., B.B.L., L.N.H.), and the Department of Mechanical and Aerospace Engineering (B.B.L., M.J.G., A.A.D.), State University of New York at Buffalo, Buffalo, New York, and the Section of Interventional Neuro-radiology (A.K.W.), University of Miami School of Medicine, Miami, FL.

This work was supported in part by Whitaker Foundation Biomedical Engineering Research grant 95-0028, a grant from Toshiba Corporation, and by a Grant from the John R. Oishei Foundation.

Address reprint requests to Ajay K. Wakhloo, MD, PhD, Section Interventional Neuroradiology (R 109), Department of Radiology, University of Miami School of Medicine, 1611 NW 12th Avenue, WW 279, Miami, FL 33136.

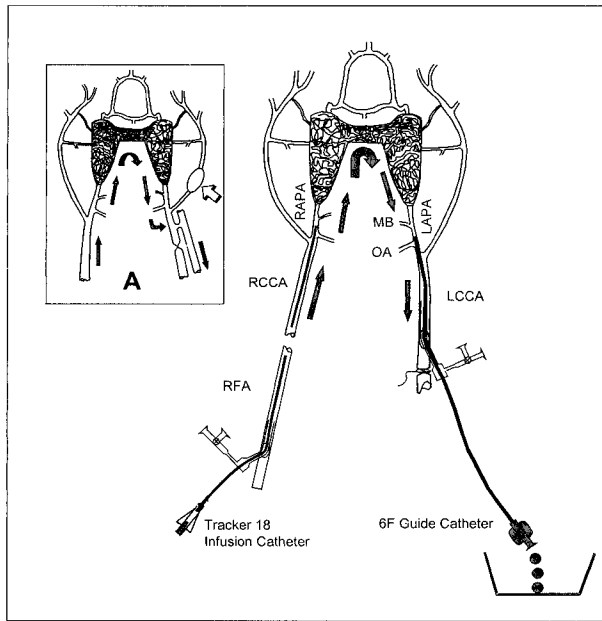


Fig 1. Schematic illustration of the simplified AVM model in swine. Large arrows indicate the direction of blood flow through the rete mirabile. A 6F-guide catheter is tightly fit into the left APA beyond the origin of the OA and serves as the venous segment of the AVM model. The CCA is surgically ligated proximal to the guide catheter. The proximal end of the catheter is opened to reduce the pressure and drives the blood toward the collection basin. A microcatheter placed in the right APA serves as the arterial side of the AVM model (Note.—RCCA = right CCA; RAPA = right APA; RFA = right femoral artery; MB = muscular branch of the APA).

The inset (A) shows the surgical preparation of the AVM model in swine as previously described by Massoud et al (1). The arteriovenous fistula and the endovascularly placed balloon within the ECA (empty arrow) promotes the blood flow from the right APA into the left jugular vein (arrows).

on average 4.2 months old (range, 3–6 months old) and of both sexes. The average weight of the Mini Yucatan swine was 32 kg (range, 30–36 kg) and of the Barnyard was 38 kg (range, 27–108 kg). All pigs were maintained on a standard laboratory diet. After an overnight fast, each swine was premedicated with an intramuscular administration of 3 mL/100 kg of Telazol and Xylazine and a subsequent intramuscular injection of 0.02 mg/kg of Atropine. General anesthesia was maintained with spontaneous ventilation or mechanical inhalation of 2% to 3% isoflurane or both via nose cone or endotracheal intubation. During the procedure, ECG and systemic blood pressure were monitored.

Under general anesthesia the femoral artery was punctured by means of Doppler sonography guidance and the modified Seldinger technique. A 7F-introducer sheath was placed into the groin. After heparinization with an initial bolus of 100 U/kg, we inserted a 6F-angled Envoy guiding catheter (Cordis Endovascular Systems, Miami, FL) into the right common carotid artery (CCA), obtaining angiograms in anteroposterior projections. Based on experience in humans, heparin infusions were adjusted to the bodyweight of the animal and the half-life of the drug to maintain a 2- to 3-times the baseline value of activated clotting time (ACT). ACTs, however, were not obtained. We used Ioxilan 62% 300 mgI/mL (Oxilan 300; Cook, Bloomington, IN) as a contrast agent. The selective angiograms through the diagnostic catheters were performed using 8 mL of pure contrast agent for the CCA, 4 mL for the ascending pharyngeal artery (APA), and 1–3 mL for the APA angiogram through the microcatheters. For the image acquisi-

tion, an Angiorex system (Toshiba, Japan) was used at a frame rate of 3.75 and 7.5 frames per second.

Subsequently, a surgical dissection of the left CCA was performed. A 7F-introducer sheath was placed after puncturing the CCA at the midcervical level proximal to the APA's origin. The CCA was ligated proximal to the sheath. Diagnostic angiograms of the CCA in anteroposterior and oblique projections were obtained. A 6F Envoy guiding catheter with an angled or straight tip was inserted tightly into the origin of the APA beyond the origin of the occipital artery (OA) (Fig 1). In three animals, a temporary balloon occlusion was performed instead of a surgical ligation of the CCA. After placing a 10F-introducer sheath into the left common femoral artery, a 10-mm nondetachable 9.4F balloon catheter (Medtronic Zeppelin Micro Interventional Systems, Sunnyvale, CA), with a maximum inflation volume of 0.8 mL, was inflated with a solution of contrast agent and saline (1:1 by volume). The 6F Envoy catheter was inserted through the balloon catheter and placed into the APA, as described above (Fig 2A and B). Contrast medium was injected through the 6F Envoy to obtain an optimal angiographic view of the rete. A submentooccipital projection was used for optimal delineation of the rete. The vascular anatomy of the rete was frequently visualized to rule out catheter-induced vasospasm. Vasospasm was frequently observed at the origin of the APA and in its entire length up to the rete. Small amounts of papaverin hydrochloride (between 12 and 18 mg, dependent on the weight of the pig) diluted in 20 mL of saline was slowly infused over 15 to 20 minutes by using a Harvard infusion pump (Harvard Apparatus Model 22, Southatic, MA). Repeat angiography was performed to document the effect of papaverin. Intravascular pressure measurements on both sides of the rete were performed only after complete resolution of the spasm. A CODMAN MicroSensor Intracranial Pressure (ICP) transducer (Johnson & Johnson Professional, Inc., Raynham, MA) was used to monitor the pressure. The transducers were placed in the right CCA close to the origin of the APA, in the left APA, and connected to an ICP Express pressure measurement unit. To determine the blood flow across the rete, we collected a blood sample through the 6F-guide catheter from the left APA over a period of 30 seconds. Subsequently, the collected heparinized blood was reinjected through the femoral sheath. A FasTracker18 microcatheter (Target Therapeutics, Fremont, CA) was then introduced into the right APA through the guide catheter and superselective angiograms were obtained with and without opening the 6F-guide catheter in the left APA that served as the venous drainage.

In the last three animals, we injected 3 mL of contrast agent by using a microinjector pump that was designed and manufactured by the senior authors (patent pending). These injections were performed at an injection speed of 1 mL/s and a maximum pressure of 20 atm (Fig 3A and B). The purpose of these micropump injections was to exclude any examiner-dependent influence on angiographic visualization of the rete by changes in injection pressure.

Results

The endovascular and combined surgical-endovascular construction of the AVM was successful in all 29 animals. Two animals did not survive for reasons unrelated to the technical aspects of the procedure. In all survivors, a pressure gradient across the AVM nidus (rete) could be found. The mean pressure gradient was 14.9 ± 10.5 mm Hg (range, 4–42 mm Hg). The mean flow across the retia was 30.4 ± 14.2 mL/min (range, 3.5–46 mL/min). The filling of the guiding catheter, representing the venous drainage of the model, was seen on

FIG 2. A, Left APA angiogram in right oblique projection obtained using a 6F catheter after occlusion of the CCA with a nondetachable 9.4F balloon catheter. The contrast agent injection was performed to demonstrate the complete occlusion of the CCA and the ECA with the balloon and the exact placement of the 6F guiding catheter within the APA.

B, Nonsubtracted angiogram of the same animal as in A shows the contrast agent-filled occlusive balloon in the left CCA.

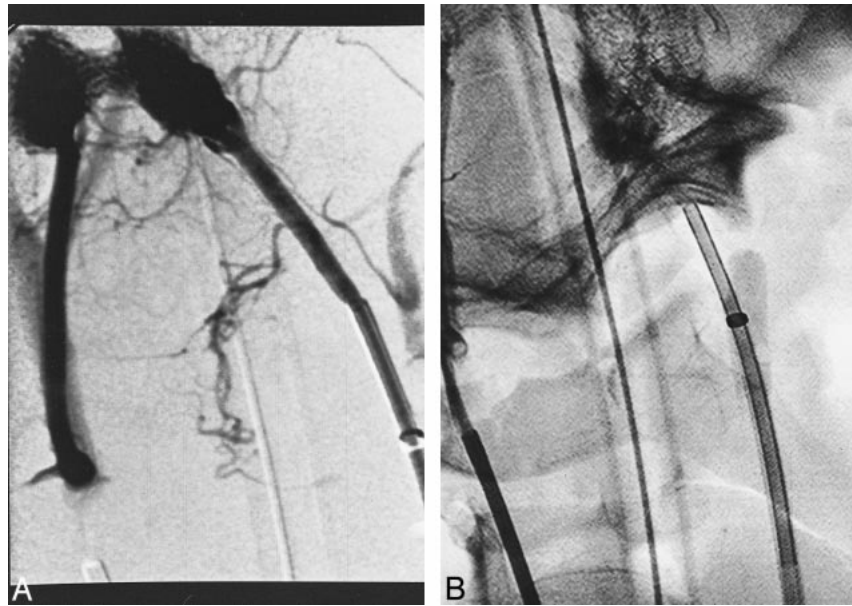
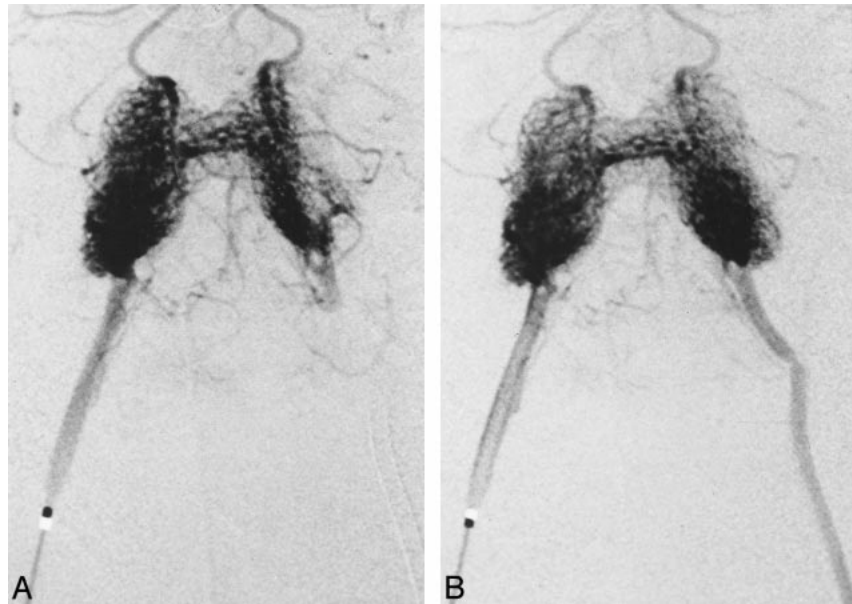


FIG 3. A, Right APA angiogram in anteroposterior and submentooccipital projection of the arteriovenous shunt through the rete mirabile. Contrast material was administered using an injector pump with preset parameters (injection speed, 1 mL/s; maximal injection pressure, 20 atm). There is a complete opacification of the ipsilateral (right) and only a partial opacification of the contralateral (left) rete.

B, Angiogram after opening the draining catheter on the left side; same animal and same injection parameters as in A. The left APA is apparent and the contrast agent-filled guide catheter represents the extended venous segment of the AVM.



angiograms only after opening the catheter hub and draining the blood.

Discussion

The swine rete is a valuable model because of its similarity to the vascular network of a plexiform human AVM. The pressure drop across the swine AVM model is commonly achieved through the surgical creation of a large carotid-jugular fistula on one side (1). Although the model has proven to be extremely useful, there are some drawbacks. The creation of an arteriovenous fistula is a time-consuming procedure, requiring both surgical and endovascular skills. Furthermore, as described by Massoud et al in the original article regarding the AVM model in the swine (1), endovascular occlu-

sion of at least three vessels is necessary (the muscular branch of the APA, the OA, and the external carotid artery [ECA]). One of the goals of our combined surgical-endovascular and endovascular approach alone was to simplify this model. The tight insertion of the 6F-guiding catheter into the origin of the APA on the venous side eliminated the need to create an arteriovenous fistula. After opening the catheter hub to the atmospheric pressure, an average pressure gradient of 14.9 mm Hg was measured, a significantly smaller value than recently reported by Murayama et al in their swine AVM model (8). Prior to embolization, they found a mean pressure of 79.5 mm Hg in the arterial feeder, whereas the mean pressure in the draining vein measured 52.0 mm Hg, yielding an average pressure gradient of approximately 27 mm Hg. They

also reported an average mean velocity of 39.3 cm/s in the draining vein prior to embolization. In comparison, we measured a mean flow of 30.4 mL/min, corresponding to a cross-sectional mean velocity of 22 cm/s and instantaneous velocity up to 44 cm/sec on average (1.7 mm inner diameter of the guiding catheter used) (9, 10). The discrepancy in findings could be related to differences between the two studies in residual perfusion of the brain via the rete. Blood flow velocities in our rete AVM model corresponded well with values found in feeding arteries and draining veins of human cerebral AVM, as recently reported (11–13).

There are three major advantages to the proposed model: 1) The combined surgical-endovascular approach is easier to create and, thus, saves time. 2) This model does not require selective occlusion of the OA, the muscular branch of the APA, and the ECA. 3) The model mimics hemodynamic parameters of human cerebral AVMs.

The original report by Massoud et al describes the ECA being occluded by using a hand-tied or Goldvalve detachable balloon, whereas the two branches of the APA were occluded by placing simple coils or endovascular unipolar electrocoagulation via the microguidewire. Our AVM model, however, can at this point only be used for acute studies (14).

Conclusion

Our simplified AVM model in swine is easier to construct than are current AVM models. It can be performed as a combined surgical and endovascular technique as well as an endovascular approach alone. Hemodynamic data, similar to the human cerebral AVM, can be obtained to characterize the arteriovenous shunt. Nonetheless, this model has only been evaluated in acute preparation and for interventional training, and the understanding of n-butyl 2-cyanoacrylate kinetics.

Acknowledgments

We wish to thank Ann Marie Paciorek for her expert technical assistance and Dagmar Schnau for editorial help.

References

1. Massoud TF, Ji C, Vinuela F, et al. **An experimental arteriovenous malformation model in swine: Anatomic basis and construction technique.** *AJNR Am J Neuroradiol* 1994;15:1537–1545
2. Chaloupka JC, Vinuela F, Sakai N, Vinters HV, Robert J, Duckwiler GR. **Potential toxic effects of superselective injection of amobarbital sodium on microvasculature: a study in an animal model.** *AJNR Am J Neuroradiol* 1994;15:1529–1536
3. Lee DH, Wriedt CH, Kaufmann JC, Pelz DM, Fox AJ, Vinuela F. **Evaluation of three embolic agents in pig rete.** *AJNR Am J Neuroradiol* 1989;10:773–776
4. Lylik P, Vinuela F, Vinters HV, et al. **Use of a new mixture for embolization of intracranial vascular malformations. Preliminary experimental experience.** *Neuroradiology* 1990;32:304–310
5. Massoud TF, Ji C, Vinuela F, et al. **Laboratory simulations and training in endovascular embolotherapy with a swine arteriovenous malformation model.** *AJNR Am J Neuroradiol* 1996;17:271–279
6. Massoud TF, Ji C, Guglielmi G, Vinuela F. **Endovascular treatment of arteriovenous malformations with selective intranidal occlusion by detachable platinum electrodes: technical feasibility in a swine model.** *AJNR Am J Neuroradiol* 1996;17:1459–1466
7. Murayama Y, Vinuela F, Ulhoa A, et al. **Nonadhesive liquid embolic agent for arteriovenous malformations: Preliminary histopathological studies in swine rete mirabile.** *Neurosurgery* 1998;43:1164–1175
8. Murayama Y, Massoud TF, Vinuela F. **Hemodynamic changes in arterial feeders and draining veins during embolotherapy of arteriovenous malformations: an experimental study in a swine model.** *Neurosurgery* 1998;43:96–104
9. Fung YC. **Biomechanics—Circulation.** *Blood Flow in Arteries.* New York: Springer Verlag;1997:108–200
10. McDonald DA. **Blood flow in arteries. The Nature of Flow of a Liquid.** 2nd ed. Baltimore MD: Williams & Wilkins;1974: 11–53
11. Lieber BB, Wakhloo AK, Divani A, Rudin S. **Determination of vascular geometry and flow velocity in cerebral arteriovenous malformations (AVMs) using double contrast and high-speed digital subtraction angiography.** *Advances in Bioengineering* 1998;34:53–54
12. Rudin S, Wakhloo AK, Lieber BB, et al. **Blood flow path and velocity measurements for cerebral arteriovenous malformations using biplane digital angiographic droplet tracking.** *AJNR Am J Neuroradiol* 1999;20:1110–1114
13. Wakhloo AK, Lieber BB, Rudin S, Duffy-Fronckowiak M, Mericle RA, Hopkins LN. **A novel approach to flow quantification in brain arteriovenous malformations prior to embolization: use of insoluble contrast (Ethiodol droplet) angiography.** *J Neurosurg* 1998;89:395–404
14. Wakhloo AK, Lieber BB, Divani A, et al. **The effect of glacial acetic acid on the kinetics of n-butyl 2-cyanoacrylate embolization in a chronic swine arteriovenous model.** Annual Joint Meeting, ASNR/ASHNR/ASPNR/ASITN/ASSR, San Diego, May 22–28, 1999